Proc. 3rd J-PARC Symposium (J-PARC2019)
JPS Conf. Proc. **33**, 011093 (2021)
https://doi.org/10.7566/JPSCP.33.011093

Commissioning of Versatile Compact Neutron Diffractometer (VCND) at the B-3 Beam Port of Kyoto University Research Reactor (KUR)

Kazuhiro MORI[1*], Ryo OKUMURA[1], Hirofumi YOSHINO[1], Masaya KANAYAMA[1], Setsuo SATOH[2], Yojiro OBA[3], Kenji IWASE[4], Haruhiro HIRAKA[5], Masahiro HINO[1], Tadafumi SANO[1], Yuji KAWABATA[1], Takashi KAMIYAMA[2], Toshiya OTOMO[2], and Toshiharu FUKUNAGA[6]

[1]*Institute for Integrated Radiation and Nuclear Science, Kyoto University, 2–1010 Asashiro-Nishi, Kumatori-cho, Sennan-gun, Osaka 590-0494, Japan*
[2]*Institute of Materials Structure Science, High Energy Accelerator Research Organization, 1–1 Oho, Tsukuba, Ibaraki 305-0801, Japan.*
[3]*Materials Science Research Center, Japan Atomic Energy Agency, Tokai, Ibaraki 319-1195, Japan*
[4]*Department of Materials Science and Engineering, Ibaraki University, 4-12-1 Nakanarusawa, Hitachi, Ibaraki 316-8511, Japan*
[5]*Neutron Science Center, Korea Atomic Energy Research Institute, Daejeon 34057, Korea*
[6]*Office of Society-Academia Collaboration for Innovation, Kyoto University, Uji, Kyoto 611-0011, Japan*

**E-mail: kmori@rri.kyoto-u.ac.jp.*

(Received November 16, 2019)

Owing to successful promotion of the research and education by Kyoto University Research Reactor (KUR), a versatile compact neutron diffractometer (VCND) was designed and built at the B-3 beam port of KUR. With a monochromatic beam of neutrons (wavelength, $\lambda = 1.0$ Å), neutron diffraction data can be collected in the scattering angle, 2θ, range of 5–130°. The resolution of the VCND, $\Delta d/d$, is approximately 1%, evaluated from the neutron diffraction data of diamond powder. As the first results of the VCND, we demonstrated structural analyses of the following energy storage materials and functional materials: strontium fluoride (SrF_2), lanthanum-nickel intermetallic alloy ($LaNi_5$), and an austenitic-ferritic stainless steel.

KEYWORDS: Neutron diffractometer, Structural analysis, Rietveld refinement, Neutron diffraction, Research reactor

1. Introduction

Kyoto University Research Reactor (KUR), which is operated at the rated thermal power of 5 MW, has long been dedicated to many types of experimental studies, including physics, chemistry, biology, engineering, agriculture, and medicine [1]. In particular, the neutron beams generated by KUR have been used for neutron diffraction (ND), small-angle neutron scattering, neutron devices estimation, and neutron imaging (or neutron radiography) experiments. A four-circle single-crystal ND (4CND) was previously installed at the B-3 beam port of KUR. For the last decade, however, the research activity using the 4CND has been quite low due to old age and the limited beam time (i.e., the period of operation on KUR is approximately 52 hours). As ND is a powerful tool to precisely determine the atomic positions of light elements (e.g., hydrogen, lithium, fluorine, and oxygen), and neutrons can penetrate deeply into materials, there is a growing demand for structural investigations of energy storage materials and functional materials, such as rechargeable batteries, hydrogen absorbing materials, and steel materials. For this reason, instead of the 4CND, a versatile compact neutron diffractometer (VCND) was built at the B–3 beam port of KUR. This article reports the design, construction, operation parameters, and first results of the VCND.

2. Instrument Design and Features

The initial design and current status of the VCND are shown in Figs. 1(a), (b), (c), and (d). Here, the VCND is viewing a light-water moderated tank on KUR. A primary collimator made of B_4C grit mixed with resin is installed; the viewing face is 55 mm × 55

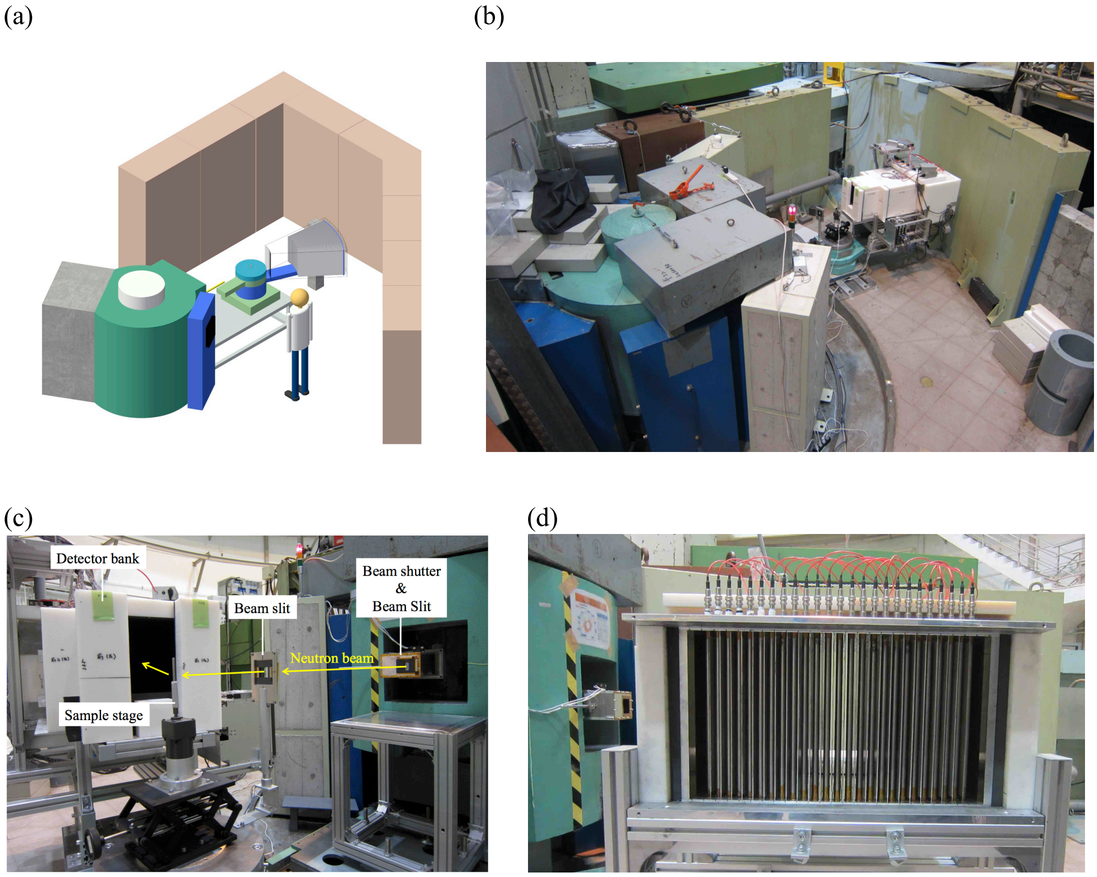

Fig. 1. Versatile compact neutron diffractometer (VCND) installed at the B-3 beam port of Kyoto University Research Reactor (KUR): (a) Initial design, (b) bird's-eye-view photograph, and (c) partial view (around the sample stage) of the VCND; (d) Detector bank including 25 ^{3}He gas-filled tube detectors (0.5-in diameter).

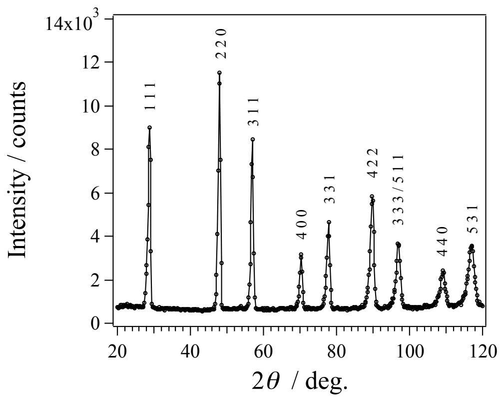

Fig. 2. Neutron diffraction data of diamond (C) powder at room temperature in the 2θ range of 20–120°, measured using the VCND.

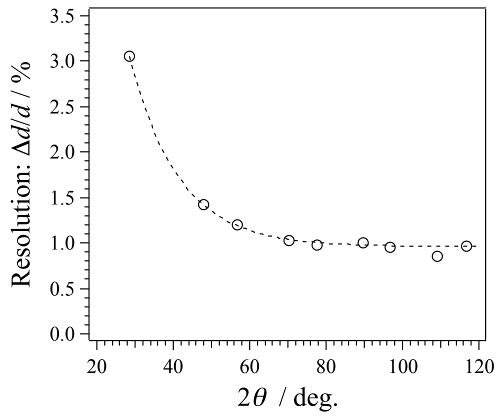

Fig. 3. Resolution of the VCND as a function of 2θ, evaluated from the neutron diffraction data of diamond (C) powder at room temperature.

mm. The Cu monochromator with 40-mm diameter of the 4CND was used on the VCND. The neutron wavelength, λ, which is monochromatized by the (220) plane of a Cu single crystal, is 1.0 Å [2]. The Cu monochromator can be controlled using a two-axis goniometer system (RA07A-W and SA05B-RM, Kohzu Precision Co., Ltd.). In Fig. 1(c), the VCND is equipped with a beam shutter and two beam slits, manufactured by the KURNS factory. The beam size is approximately 10 mm in width and 30 mm in height. For operation at the power of 5 MW on KUR, the beam flux, ϕ, is 1.3×10^5 n/s/cm^2 at the beam shutter, estimated by the gold foil activation method. The distance from the Cu monochromator to the sample is approximately 2 m, and the distance from the sample to the detector is 1.2 m. A detector bank including 25 ^{3}He gas-filled tube detectors (0.5-in diameter) is placed on an arm of the HUBER-440 goniometer. Using the detector bank, we can measure the ND data in the 2θ range of 5–130°, where 2θ is the scattering angle. It is worth noting that the neutron encoding with the high speed network NEUNET-c module has been introduced to the VCND [3]. Therefore, we can store the ND data as the event mode. The resolution of the VCND, $\Delta d/d$, is approximately 1%, evaluated from the ND data of diamond (C) powder, as shown in Figs. 2 and 3.

3. First Results of VCND

3.1 Strontium fluoride (SrF_2)

Strontium fluoride (SrF_2) is a key material for the solid electrolytes of all-solid-state fluoride-ion batteries [4]. The crystal structure of SrF_2 is well-known as the fluorite-type structure, comprising a metal site and a fluorine site: Sr(0, 0, 0) in the 4*a* site and F(1/4, 1/4, 1/4) in the 8*c* site (Wyckoff notation in space group $Fm\bar{3}m$). To assess the ability of the VCND, we performed the ND experiment using SrF_2 powder.

Figure 4(a) shows the ND data of SrF_2 at room temperature. The step interval in 2θ, $\Delta 2\theta$, was 0.2 º. The crystal structure was refined by a Rietveld-refinement program, RIETAN–FP [5]. In the figure, a good fit was obtained between the observed and calculated intensities (where the reliability factor R_{wp} = 7.129%, and the goodness-of-fit

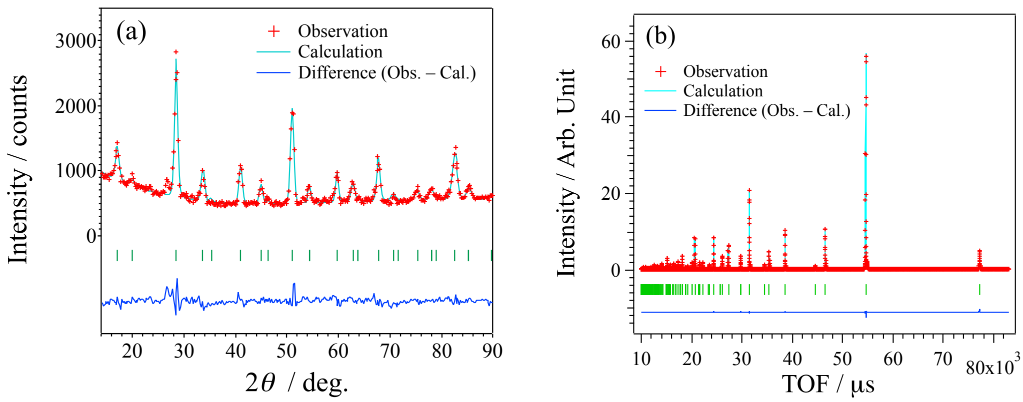

Fig. 4. Rietveld refinements using neutron diffraction (ND) data for SrF_2, measured by (a) VCND (KURNS) and (b) SPICA (J-PARC MLF). The plus marks (red) indicate the observed ND data, while the solid lines (light blue) indicate the calculated ND data. The vertical marks (green) below the ND data denote the positions of the Bragg reflections. The curves (blue) at the bottom indicate the difference between the observed and calculated intensities.

S = 1.9136). The lattice constant, a, was estimated to be 5.85(15) Å. The isotropic atomic displacements of Sr and F, B_{iso}(Sr) and B_{iso}(F), were determined as 0.39(16) and 0.77(15) $Å^2$, respectively. In addition, the time-of-flight (TOF) ND analysis of SrF_2 was performed using the special environment neutron diffractometer, SPICA, located at the BL09 beam port of the Materials and Life Science Experimental Facility, Japan Proton Accelerator Research Complex (J–PARC MLF) [6], and the suite of analysis programs called Z-Rietveld (see Fig. 4(b)) [7,8]. The values of a, B_{iso}(Sr), and B_{iso}(F) were refined as follows: a = 5.800235(7) Å, B_{iso}(Sr) = 0.5403(18) $Å^2$, and B_{iso}(F) = 0.8183(19) $Å^2$ (where R_{wp} = 3.4793% and S = 1.9681). Consequently, the a, B_{iso}(Sr), and B_{iso}(F) values obtained from the VCND were in good agreement with those obtained from the SPICA. In particular, we confirmed the reliability of the atomic displacement parameters obtained from the VCND.

3.2 Lanthanum-nickel intermetallic alloy ($LaNi_5$)

The lanthanum-nickel intermetallic alloy ($LaNi_5$) is best known as an excellent hydrogen-absorbing material [9,10]. Figure 5 shows the Rietveld refinement using the ND data for $LaNi_5$ at room temperature, where $\Delta 2\theta = 0.1°$. In the Rietveld analysis, the atomic positions, La (0, 0, 0) in the 1a site, Ni1 (1/3, 2/3, 0) in the 2c site, and Ni2 (1/2, 0, 1/2) in the 3g site, were used to refine its crystal structure based on the space group $P6/mmm$ (hexagonal system). As a result, the values of a and c were

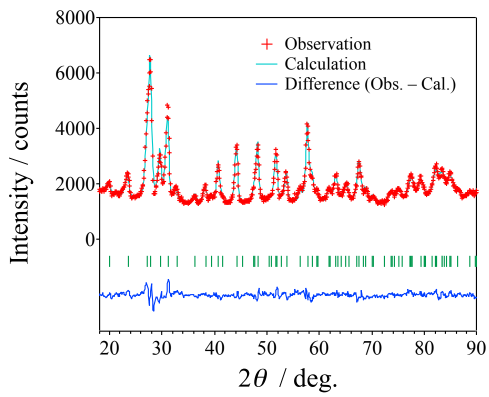

Fig. 5. Rietveld refinement using ND data for $LaNi_5$ at room temperature.

estimated to be 5.04(7) and 4.01(4) Å (where R_{wp} = 4.981% and S = 2.2130); which agree with literature data [10]. The B_{iso} value was also determined for each element: B_{iso}(La) = 0.43(9), B_{iso}(Ni1) = 0.65(7), and B_{iso}(Ni2) = 0.19(6) Å^2.

3.3 Austenitic-ferritic stainless steel

Austenitic-ferritic stainless steels (generally known as duplex stainless steels) are used in a wide range of applications, including for equipment in chemical plants, oil plants, and food-processing. This is because they possess higher toughness, strength, and corrosion resistance. The Austenitic-ferritic stainless steel comprises two phases: austenitic phase with the face-centered cubic (fcc) structure and ferritic phase with the body-centered cubic (bcc) structure.

Figure 6(a) shows a screw of the austenitic-ferritic stainless steel (SUS329J4L). The ND data of the SUS screw were collected with five different 2θ ranges (hereafter referred to as "Frames") using the detector bank including 25 ^{3}He gas-filled tube detectors: (Frame-1) 20–44.8°, (Frame-2) 40–64.8°, (Frame-3) 60–84.8°, (Frame-4) 80–104.8°, and (Frame-5) 100–124.8°, where $\Delta 2\theta$ = 0.2 °. The measurement time for each frame was 25 minutes at the power of 1 MW on KUR. Figure 6(b) displays the combined ND data of the SUS screw and its total measurement time was 125 minutes (= 25 minutes × 5 frames). In the figure, the fcc and bcc phases could be confirmed. Furthermore, the difference between the ND data of the SUS screw without and with rotation was clearly observed owing to the preferred orientations of the fcc and bcc phases. Thus, the VCND is applicable for studying the mechanical properties of stainless-steel materials regarding the formation of the textures. For example, the texture data of ND for one frame can be measured for several minutes using the VCND when KUR is operated at the power of 5 MW.

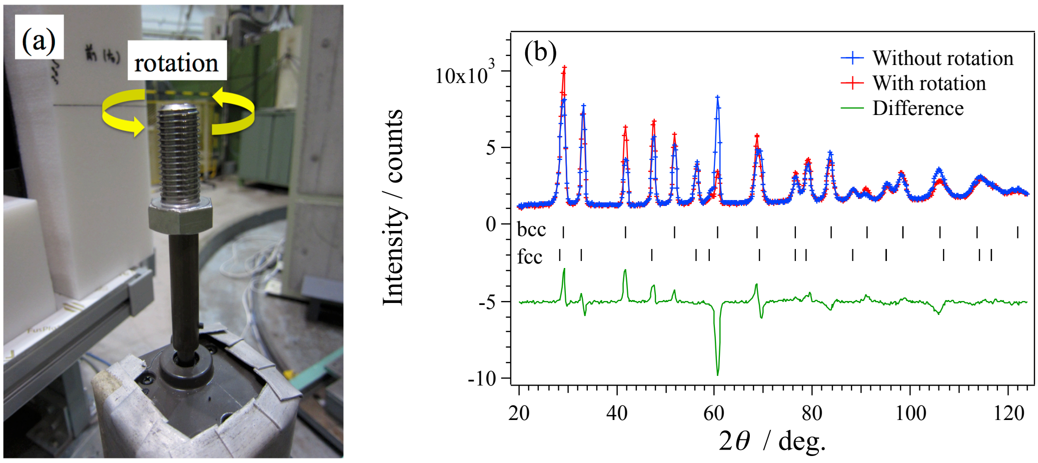

Fig. 6. (a) Screw of the austenitic-ferritic stainless steel (SUS329J4L) placed on the sample stage of the VCND. (b) ND data of the SUS screw. The plus marks indicate the observed ND data of the SUS screw without rotation (blue) and with rotation (red). The vertical marks (black) below the ND data denote the positions of the Bragg reflections for the bcc and fcc phases. The curve (green) at the bottom indicates the difference between the ND data of the SUS screw without and with rotation.

4. Conclusions

The VCND was designed and built at the B-3 beam port of KUR. We reported its specifications, particularly the neutron wavelength, λ, of 1.0 Å, the neutron beam flux, ϕ, of 1.3×10^5 n/s/cm^2 (for operation at the power of 5 MW on KUR), and the resolution of the VCND, $\Delta d/d$, as approximately 1%. The first results of the VCND were shown for SrF_2, $LaNi_5$, and an austenitic-ferritic stainless steel. Although the $\Delta d/d$ value of the VCND was somewhat large, we could obtain reasonable structural parameters in the Rietveld refinements. The improvements of the VCND make KUR extremely useful for successful promotion of the research and education. Further developments, including environmental equipment, are now in progress.

Acknowledgments

The authors acknowledge Dr. Muto of KEK for his help with the installation of a data acquisition system. We thank Ms. Mori for her help with the schematic design of the VCND. The ND experiments were performed at the B-3 beam port of KUR with the approval of the Institute for Integrated Radiation and Nuclear Science, Kyoto University (KURNS) (Proposal No. 30064 and 31016). The TOF-ND experiments were approved by the Neutron Scattering Program Advisory Committee of Institute of Materials Structure Science, High Energy Accelerator Research Organization (IMSS, KEK) (Proposal No. 2019S10). This work was partially supported by the Japan Society for the Promotion of Science (JSPS) KAKENHI Grant Number: 19H02457.

References

[1] For current information on KUR see: https://www.rri.kyoto-u.ac.jp/en/facilities/kur
[2] For example, M. Machida, Y. Tamura and M. Komukae: KURRI Prog. Rep. 2004, 5 (2005).
[3] S. Satoh, S. Muto, N. Kaneko, T. Uchida, M. Tanaka, Y. Yasu, K. Nakayoshi, E. Inoue, H. Sendai, T. Nakatani and T. Otomo: Nucl. Instrum. Methods Phys. Res., Sect. A **600**, 103 (2009).
[4] M.A. Reddy and M. Fichtner: J. Mater. Chem. **21**, 17059 (2011).
[5] F. Izumi and K. Momma: Solid State Phenom. **130**, 15 (2007).
[6] M. Yonemura, K. Mori, T. Kamiyama, T. Fukunaga, S. Torii, M. Nagao, Y. Ishikawa, Y. Onodera, D.S. Adipranoto, H. Arai, Y. Uchimoto and Z. Ogumi: J. Phys. Conf. Ser. **502**, 012053 (2014).
[7] R. Oishi, M. Yonemura, Y. Nishimaki, S. Torii, A. Hoshikawa, T. Ishigaki, T. Morishima, K. Mori and T. Kamiyama: Nucl. Instrum. Methods Phys. Res., Sect. A **600**, 94 (2009).
[8] R. Oishi-Tomiyasu, M. Yonemura, T. Morishima, A. Hoshikawa, S. Torii, T. Ishigaki and T. Kamiyama: J. Appl. Crystallogr. **45**, 299 (2012).
[9] Y. Nakamura, K. Ogura, I. Uehara and E. Akiba: J. Alloys Compd. **298**, 138 (2000).
[10] K. Mori, K. Iwase, Y. Oba, T. Fukunaga and M. Sugiyama: Mater. Trans. **55**, 1643 (2014).